Burst-Mode Clock and Data Recovery with FEC and Fast Phase Acquisition for Burst-Error Correction in GPONs

Bhavin J. Shastri, Julien Faucher Ming Zeng, and David V. Plant

Department of Electrical and Computer Engineering, Photonic Systems Group, McGill University

Montréal, Canada

Email: shastri@ieee.org

Abstract—We demonstrate experimentally for the first time the impact of forward error correction (FEC) on the performance of 622/1244 Mb/s burst-mode clock and data recovery (BM-CDR) with instantaneous phase acquisition (0 bit) for any phase step ($\pm 2\pi$ rads) for gigabit-capable passive optical network (GPON) optical line terminator (OLT) applications with (255, 239) Reed-Solomon (*R-S*) codes. Our design is based on commercially available SONET CDRs operated in $2\times$ over sampling mode. This burst-mode receiver (BM-RX) provides a $\sim$ 5 dB coding gain at bit error ratio (BER) of 10^{-10}. We also show that this novel technique of employing FEC on BM-CDRs with fast phase acquisition time, provides a solution for fast burst-error correction giving reliable and predictable BERs in bursty-channels. The BM-RX meets the GPON physical media dependent layer specifications defined in the ITU-T G.984.2 recommendation. The coding gain can be used to increase the optical link budget as specified in the ITU-T G.984.3 standard, that is, support higher bit rates, achieve longer physical reach between the OLT and the optical network units (ONUs), as well as increase the number of splits per single PON tree.

I. Introduction

PONs are an emerging access network technology that provide a low-cost method of deploying fiber-to-the-home. Fig. 1 shows an example of a PON network. In the upstream direction, the network is point-to-multipoint. Because upstream packets can vary in phase and amplitude due to optical path differences, the OLT requires a BM-RX and a BM-CDR. Within the OLT, the BM-RX is responsible for amplitude recovery, whereas the BM-CDR is responsible for phase recovery. This paper is about the design of a BM-CDR.
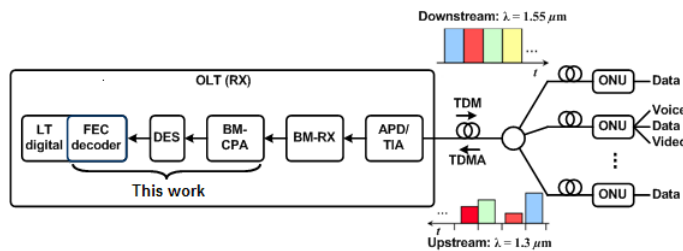

Fig. 1. Generic GPON network architecture for FTTx scenarios showing the work in context. OLT: optical line terminator; RX: receiver; LT: line terminator; FEC: forward error correction; DES: deserializer; APD: avalanche photodiode; TIA: transimpedance amplifier; TDM: time division multiplexing; TDMA: time division multiple access; ONU: optical network unit.

Current PON systems employ Fabry-Perot (FP) lasers, a multi-longitudinal mode (MLM) device, at the ONU, as it is the most cost effective solution for meeting the PON requirements - the optical power required for a 20 km reach in the $1310 - 1550$ nm range [1]. However, performance of the system may be severely impaired by the mode partition ratio (MPN) [2] of a FP laser coupled with the chromatic dispersion that exists in the transmission fiber. Thus, MPN introduces a limitation in the length of the optical link.

Another significant problem is that of burst-errors (clustered bit errors) that inherently arise in GPON channels because of the phase acquisition process by BM-CDRs for bursty data. This makes the BER measurements unreliable and unpredictable, and therefore not a true BER representation. There are two comments on this. Firstly, at a particular SNR, the BER does not converge because of the presence of burst-errors from packet to packet. Thus, the BER will change from measurement to measurement for the same SNR. Secondly, the BER will also vary for packets with different phases at the same SNR because the phase acquisition time of the CDR is a function of the relative phase between two packets.

FEC with Reed-Solomon (*R-S*) codes is useful for burst-error correction [3]. Defined as $R\text{-}S(n, k)$, R-S codes are block based as they divide a codeword of n symbols into m-bit symbols with k symbols of data and $2t = (n - k)$ symbols of parity. By definition, an $R\text{-}S(n, k)$ code has an error correcting capability of t symbol errors. The $R\text{-}S(255, 239)$ is recommended by the ITU-T G.984.3 [4] standard for GPON BM-RXs.

However, there is no guarantee that the length of burst-errors will be less than the code's error correcting capability. Burst-error correcting codes have been demonstrated for bursty channels [5]-[9], but these codes are complex and introduce latency at the circuit level implementation. Our novel technique of employing FEC with *R-S* codes on BM-CDRs with fast phase acquisition, provides a simple solution around this problem resulting in fast burst-error correction giving reliable and predictable BERs in bursty-channels. In this paper, we experimentally verify the claim of an increased optical link budget of $\sim 3-4$ dB made in the ITU-T G.984.2 standard [10].

II. EXPERIMENTAL SETUP

To test the BM-CDR with FEC and *R-S* decoding, we use the custom burst-mode test setup (BM-TS)[1] as depicted in Fig. 2 [11]. The BM-TS has two main functionalities. First, it can generate alternating packets with adjustable amplitude and phase to emulate PON traffic. Second, it can perform BER measurements. Consequently, the BER measurements can also be used to determine the amplitude/phase acquisition times, and the number of consecutive identical digits (CIDs) supported by the BM-CDR.
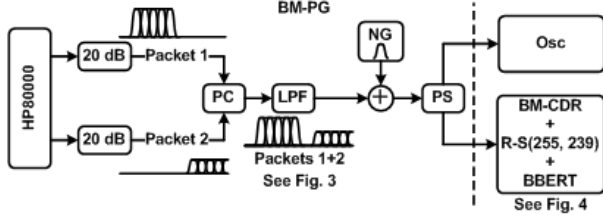

Fig. 2. Burst-mode packet generator. The burst-mode packet generator is on the left of the dashed line. When performing the BER measurements, the two packets are set to have the same amplitude. BM-PG: burst-mode pattern generator; PC: power combiner; LPF: low-pass filter (4th order Bessel-Thomson); NG: Gaussian noise generator; PS: power splitter; Osc: oscilloscope; BM-CDR: burst-mode clock and data recovery; R-S: Reed-Solomon; BBERT: burst bit error rate tester.

The BM-PG generates the upstream traffic shown in Fig. 3. Packet #1 serves as a dummy packet to force the BM-CDR to lock to a certain phase (ϕ_1) before the arrival of packet #2. The BER and phase acquisition times measurements are performed on packet #2, which consists of guard bits (16), preamble bits (0 to 2^{15}), delimiter bits (20), payload bits (2^{15}), comma bits (48), and a '1010...' pattern that can be circularly shifted in front of the delimiter to increase the preamble length. The guard, preamble, and delimiter bits correspond to the physical-layer upstream burst-mode overhead specified by the ITU-T G.984.2 standard [10]. The guard bits provide distance between two consecutive packets to avoid collisions. The preamble is used to perform amplitude and phase recovery. The delimiter is a unique pattern indicating the start of the packet to perform byte synchronization. Likewise, the comma is a unique pattern to indicate the end of the payload. The payload is an *R-S* encoded $2^{15}-1$ PRBS with a zero appended at the end. The packet loss ratio (PLR) and the BER are measured on the payload bits only. The lock acquisition time corresponds to the number of bits that need to be circularly shifted in front of the delimiter in order to get a PLR of zero for over three minutes at 622.08 Mb/s ($> 10^6$ packets received) and a BER $< 10^{-10}$.

As shown in Fig. 3, the preamble is split into two fields, a threshold determination field (TDF) for amplitude recovery and a CPA field for clock-phase recovery. In order to generate this pattern, we use two ports of an *HP80000* pattern generator

[1]The BM-TS can go up to 1 Gb/s. This limitation, which comes from the *HP80000*, explains why the design of the BM-CDR with FEC can only be experimentally verified at 622.08 Mb/s.
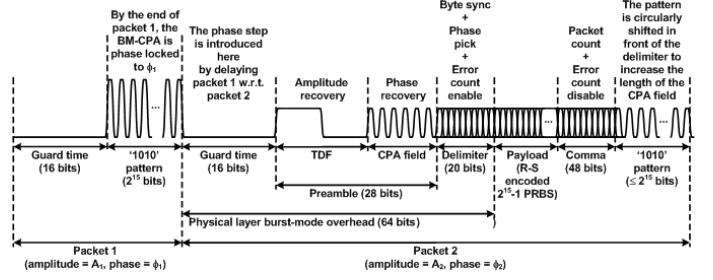

Fig. 3. Test signal and specification of the upstream burst-mode overhead. When performing BER measurements and testing the phase acquisition time, the two packets are set to have the same amplitude. TDF: threshold determination field; CPA: clock phase alignment; PRBS: pseudo-random binary sequence.

(see Fig. 2). The two packets are combined on the same line using an RF power combiner, which emulates the optical power combiner of a PON network (see Fig. 1). We use 20-dB attenuators to control the maximum amplitude of the packets and minimize reflections [12]. To test the FEC and BM-CDR under stringent conditions, we stress the input pattern in two different ways. First, we slow down the edges of the input pattern with a 4th-order Bessel-Thomson filter having a -3-dB bandwidth of 467 MHz (0.75×622 MHz) (see the LPF block in Fig. 2). Second, we add a random noise generator after the filter. The noise generator consists of a transimpedance amplifier (TIA) powered by a supply voltage approximately 1 V lower than the nominal voltage of 3.3 V. The thermal noise generated by the TIA has a Gaussian distribution, which translates into 63 ps of random jitter.

III. BURST-MODE CDR WITH FEC AND *R-S* DECODING

The main building blocks of the BM-CDR with FEC, as depicted in Fig. 4, are a SONET CDR, a byte synchronizer, a phase picker, phase-locked loops (PLLs), and an R-$S(255, 239)$ decoder. The latter three are implemented on the FPGA, alongside the BBERT. The multirate CDR is from Analog Devices (part #*ADN2819*). The deserializer is from Maxim-IC (part #*MAX3885*). Its main function is to parallelize the data as the R-$S(255, 239)$ decoder accepts one symbol (8-bit) data block every clock cycle.
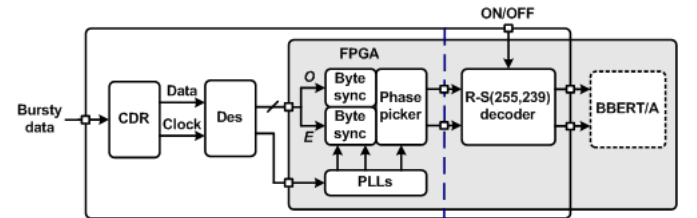

Fig. 4. Block diagram of the GPON BM-CDR with FEC. CDR: clock and data recovery; Des: deserializer; PLLs: phase-locked loops; R-S: Reed-Solomon; BBERT/A: burst bit error rate tester/analyzer; O: odd bits output of the deserializer; E: even bits output of the deserializer. Odd and even bits are a result of sampling the bursty input at t_{odd} and t_{even} sampling instants respectively.

This receiver architecture is built upon the novel burst-mode clock phase aligner (BM-CPA) [11] based on commercially available SONET CDRs operated in $2\times$ over sampling mode, which achieves instantaneous phase acquisition (0 bit) for any phase step ($\pm 2\pi$ rads). The idea behind the BM-CPA is based on a simple, fast, and effective algorithm. The odd bits of the recovered data from the CDR output are forwarded to path O and the even bits are forwarded to path E. The byte synchronizer is responsible for detecting the delimiter. The idea behind the phase picking algorithm is to replicate the byte synchronizer twice in an attempt to detect the delimiter on the odd and even samples of the data respectively. The phase picker uses feedback from the byte synchronizers to select the right path.

IV. EXPERIMENTAL RESULTS AND DISCUSSION

To study the impact of FEC on GPON BM-RXs, BER measurements are performed on the $2^{15} - 1$ PRBS payload of packet #2 (see the upstream traffic shown in Fig. 3) with and without FEC. The BM-CDR rated at $622/1244$ Mb/s is operated at $664/1327$ Mb/s to account for the $(n/k) = 15/14$ FEC overhead.

The plots in Fig. 5 show the waterfall curve - BER as a function of the input signal power when FEC is disabled and enabled. It can be observed that at an input power, P_o, of -32.5 dBm, the BER without FEC is 10^{-4} while error free operation is obtained with FEC (for same P_o). This is as expected from theory as FEC with R-$S(255, 239)$ codes are effective after BER $\geq 10^{-4}$.
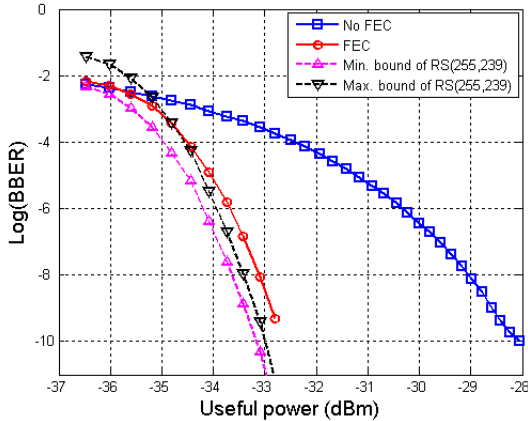

Fig. 5.   BER performance comparison of a GPON BM-CDR with FEC (red curve) and without FEC (blue curve). The theoretically obtained minimum and maximum bounds with FEC based under the assumption of purely random bit errors, are shown as well. The experimental FEC curve does not fall between these bounds based on the fact that the bit errors are not purely random and deterministic jitter is the dominating factor.

According to the ITU-T G.984.2 standard, the FEC coding gain, G, is defined as the difference input power at the receiver with and without FEC for a BER of 10^{-10}. We report a coding gain of $G = \sim 5$ dB at BER of 10^{-10} verifying the claim of the increased link budget in ITU-T G.984.3.

Burst-errors inherently arise in GPON channels because of the phase acquisition process by BM-CDRs for bursty and packet mode data, making the BER measurements unreliable and unpredictable, and therefore not a faithful representation of the true BER. R-S codes are particularly useful for burst-error correction but there is no guarantee that the length of burst-errors will be less than the codes' error correcting capability. We show in the following example, that this condition can be relaxed with a BM-CPA and R-S decoding. At the same time we also show how we achieve reliable and predictable BER with fast convergence.

With FEC disabled, from Fig. 6(a) ($P_o = -28$ dBm), it can be seen that there are bursts of errors. This effect is worsened with the BM-CPA turned off and if there exists any phase step, $-2\pi \leq \phi \leq +2\pi$ rads, between the packets, with worst being for $\phi = \pm\pi$ rads. However, with FEC enabled and BM-CPA turned on, instantaneous phase acquisition (0 bit) for any phase step ($\pm 2\pi$ rads) is achieved, consequently eliminating burst-errors and obtaining error free operation (for the same SNR) as shown in Fig. 6(b).

To further illustrate the *fast* elimination of burst-errors, we consider the following case: For a lower SNR when error free operation is not obtained with FEC, for example at $P_o = -33$ dBm, it can be observed from Fig. 6(c) that burst-errors have been eliminated with the BER curve converging quickly to the *true* and *predictable* value.

To verify this claim, we measure the waterfall curves for packets with different phases from -2π to $+2\pi$ rads. In accordance to our prediction, the waterfall curve shown in Fig. 5 is the same for any phase step between the packets. Our measurements are made on packets with no preamble bits. To achieve the same results with only a SONET CDR, 40 preamble bits are necessary as also demonstrated in [11].

To compare the experimental results with theory, consider the decoded symbol-error probability, P_E, for an R-$S(n, k) = (255, 239)$ code. It can be written in terms of the channel symbol-error probability, p [3]:

$$P_E \approx \frac{1}{2^m - 1} \sum_{j=t+1}^{2^m - 1} j \binom{2^m - 1}{j} p^j (1-p)^{2^m - 1 - j} \quad (1)$$

where $t = (n - k)/2$ is the symbol-error-correcting capability of the code. Under the assumption of purely random bit errors,

$$p = 1 - (1 - \varepsilon)^m \quad (2)$$

where ε is the channel BER without FEC as measured in Fig. 5 (blue curve). The upper and lower bounds for the channel BER with FEC, $\varepsilon_{RS(n,k)}$, as depicted in Fig. 5, are calculated using (1) and

$$\varepsilon_{RS(n,k)} = P_E \times \frac{s}{m} \quad (3)$$

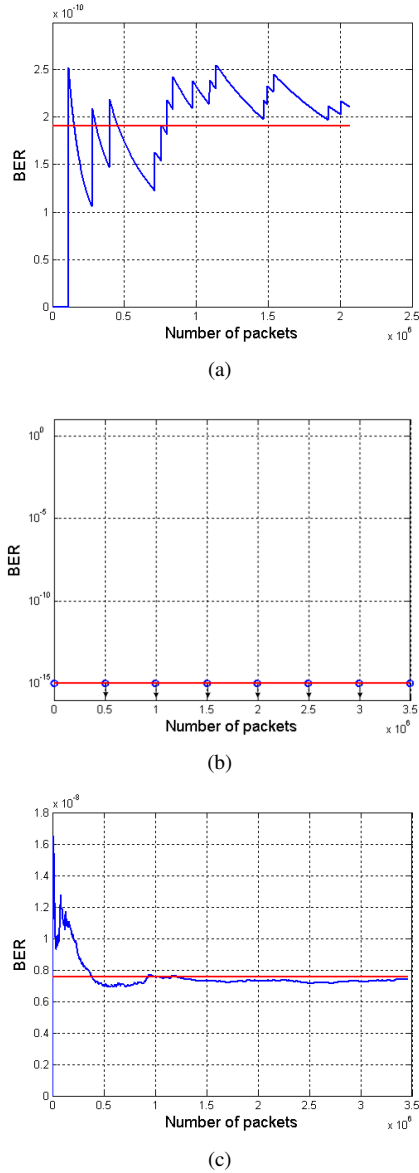where $s = m$ errors/symbol for the upper bound and $s = 1$ for the lower bound.

Fig. 6. BER as a function of time (number of packets received by the BM-CDR). (a) Without FEC (burst-errors and no BER convergence). (b) Error free operation with FEC and BM-CPA enabled for the same input power, $P_o = -28$ dBm as (a). (c) With FEC and BM-CPA enabled for a lower SNR ($P_o = -33$ dBm, elimination of burst-errors and fast BER convergence). The straight line shows the average BER over the period of packet reception. Measurements made with preamble length set to zero.

It can be observed from Fig. 5 that the experimental BER with FEC lies within these bounds for BER $< 10^{-4}$ and lies outside these bounds for BER $> 10^{-4}$. The reason for this is based on the fact the BER performance is a function of intrinsic and extrinsic effects of the channel, that is, the presence of random and deterministic jitter will affect the error correcting capability of the *R-S* codes. Since (2) and (3) assume *purely random* bit errors, the channel BER with FEC is overestimated for BER $> 10^{-4}$. This is attributed to the fact that as the SNR is increased, the presence of random jitter is attenuated relative to the presence of deterministic

jitter. Consequently, for BER $> 10^{-4}$, deterministic jitter is the dominating factor.

V. CONCLUSION

We have successfully demonstrated a $622/1244$ Mb/s BM-CDR with FEC and *R-S* codes for GPON OLT applications that meets the G.984.2 and G.984.3 specifications. This receiver provides for fast burst-error correction in bursty channels and also achieves an instantaneous phase acquisition. The coding gain obtained verifies the claim of the increased link budget by the G.984.3 standard. The coding gain can be used to reduce the minimum and maximum transmitter power by 5 dB or increase the minimum receiver sensitivity by the same amount. Alternatively, it can be used to achieve a longer physical reach or a higher split ratio when using a MLM laser in the ONU to reduce the penalty due to MPN. A novel technique for fast burst-error correction for bursty channels is also presented. This is achieved by employing FEC on BM-CDRs with fast phase acquisition time.

ACKNOWLEDGMENT

REFERENCES

[1] X. Liu, C. Lu, and T. H. Cheng, "Forward error control in passive optical networks," in *Tech. Dig. Optical Fiber Communication Conf. (OFC/NFOEC)*, Mar. 6-11, 2005, vol. 1.
[2] G. P. Agrawal, P. J. Anthony, and T. M. Shen, "Dispersion penalty for $1.3-\mu$m lightwave systems with multimode semiconductor lasers," *IEEE J. Lightwave Technology*, vol. 6, pp. 620-625, 1988.
[3] B. Sklar, *Digital communications: Fundamentals and Applications,* 2nd ed. Upper Saddle River, NJ: Prentice Hall, 2001, Chap. 5.
[4] *Gigabit-capable Passive Optical Networks (GPON): Transmission convergence Layer for Gigabit Passive Optical Networks*, ITU-T Recommendation G.984.3., 2004.
[5] D. W. Hagelbarger, "Recurrent codes: easily mechanized, burst-correcting, binary codes," *Bell Syst. Tech. J.*, 38, pp. 969-984, July 1959.
[6] I. Wadare, "On type B1 burst-error correcting convolutional codes," *IEEE Trans. Inf. Theory*, IT-14, pp. 577-583, July 1968.
[7] A. D. Wyner and R. B. Ash, "Analysis of recurrent codes," *IEEE Trans. Inf. Theory*, IT-9, pp. 143-156, July 1963.
[8] E. R. Berlekamp,"Notes on recurrent codes," *IEEE Trans. Inf. Theory*, IT-10, pp. 257-258, July 1964.
[9] A. Kohlenberg and G. D. Forney, Jr., "Convolutional coding for channels with memory," *IEEE Trans. Inf. Theory*, IT-14, pp. 618-626, July 1968.
[10] *Gigabit-capable Passive Optical Networks (GPON): Physical Media Dependent (PMD) layer specification*, ITU-T Recommendation G.984.2., 2003.
[11] J. Faucher, M. Mukadam, A. Li, and D. V. Plant, "622/1244 Mb/s burst-mode CDR for GPONs," *IEEE. Conf. Laser and Electro Optics*, pp. 420-421, Montréal, Canada, Oct. 2006.
[12] Fixed attenuators help minimize impedance mismatches. Mini-Circuits application note AN-70-001 [Online]. Available: http://www.minicircuits.com/appnote/an70001.pdf.